

GaAs-based self-aligned laser incorporating InGaP opto-electronic confinement layer

K.M. Groom, B.J. Stevens, D.T. Childs, R.R. Alexander, A.B. Krysa, J.S. Roberts, A.S. Helmy and R.A. Hogg

The realisation of GaAs-based self-aligned lasers based on a single overgrowth, and avoiding exposure of AlGaAs during fabrication, is demonstrated. An *n*-doped InGaP layer is utilised for both electrical and optical confinement, resulting in single lateral mode emission from an $\text{In}_{0.17}\text{Ga}_{0.83}\text{As}$ double quantum well laser.

Introduction: Lasers based on the GaAs materials system offer advantages over their InP counterparts, such as the use of larger substrates (>three inches) and a larger conduction band offset enabling higher temperature, uncooled operation. However, GaAs edge-emitting lasers are only available commercially as simple Fabry-Pérot ridge or oxide stripe structures. Such structures suffer from surface recombination, carrier spreading and poor fibre coupling efficiencies. Buried heterostructures and self-aligned stripes (e.g. [1]) are utilised in the manufacture of InP datacomms lasers yielding: high reliability; small active widths and control of carrier flow; high-quality interfaces; and reduced non-radiative recombination at exposed surfaces. The flexibility provided by this approach also affords greater control and stability of the optical beam profile.

Epitaxial regrowth in GaAs-based structures is problematic owing to the Al-containing layers within the structure which, when exposed to oxygen, result in poor regrowth interfaces. Previous solutions have included the use of: Al-free epitaxial structures [2]; steam oxidation [3]; *in situ* etching and regrowth [4]; and antiguided [5] or buried ridge [6] structures, in which Al layers are exposed to oxygen. All these have associated difficulties in process control, reliability, and design flexibility. In this Letter, we present a novel technique for fabrication of GaAs-based self-aligned lasers utilising an *n*-doped InGaP current blocking layer that also provides optical confinement. This technology relies on the careful design of the epitaxial structure to ensure that no $\text{Al}_x\text{Ga}_{1-x}\text{As}$ is exposed during the fabrication process. In this work we utilise a ~ 980 nm quantum well active region design. However, the technology would be well suited for exploitation of long wavelength quantum dot and dilute nitride technology for application in metro and access datacomms.

Device design & fabrication: A schematic representation of our completed device is shown in Fig. 1a. The *p-n-p-n* current blocking layers also provide a refractive index contrast with the stripe region in order to provide optical and carrier confinement simultaneously.

The initial MOVPE epitaxial growth was carried out on a 3° -off (100) n^+ GaAs substrate. Following the growth of a GaAs buffer, 1000 nm Si-doped $\text{Al}_{0.42}\text{Ga}_{0.58}\text{As}$ (doping concentration of $5 \times 10^{17} \text{ cm}^{-3}$) lower cladding was grown. The double quantum well (DQW) active region comprises two $\text{In}_{0.17}\text{Ga}_{0.83}\text{As}$ quantum wells separated by 20 nm GaAs, grown within a 100 nm GaAs separate confinement heterostructure. Above the active region 300 nm $\text{Al}_{0.42}\text{Ga}_{0.58}\text{As}$ (C-doped $5 \times 10^{17} \text{ cm}^{-3}$) was grown before a 600 nm lattice matched *n*-doped InGaP layer (Si-doped $5 \times 10^{17} \text{ cm}^{-3}$) was sandwiched between two undoped 10 nm GaAs layers. The lower GaAs layer prevents the exposure of $\text{Al}_{0.42}\text{Ga}_{0.58}\text{As}$ to oxygen during the fabrication process and acts as an etch stop, and the upper GaAs layer prevents an exchange interaction between P and As during the subsequent regrowth step.

The planar wafer was patterned and wet chemically etched (*ex situ*) into 1, 2, 3 and $5 \mu\text{m}$ -wide stripes, leaving a smooth GaAs surface at the bottom of the stripe. Prior to regrowth the wafer was cleaned in 1% buffered HF. The regrowth process consisted of ramping up to the growth temperature in an arsine environment, before the growth of 100 nm GaAs (C-doped $5 \times 10^{17} \text{ cm}^{-3}$), 1000 nm $\text{Al}_{0.42}\text{Ga}_{0.58}\text{As}$ (C-doped from 5×10^{17} to $1 \times 10^{18} \text{ cm}^{-3}$), and a 200 nm GaAs contact layer (C-doped $2 \times 10^{19} \text{ cm}^{-3}$). The material was etched into $50 \mu\text{m}$ wide ridges for electrical isolation, and AuZnAu (top) and InGeAu (back) contacts were applied. 1 mm bars were left uncoated and mounted epi-side-up on AlO_2 tiles for characterisation.

A cross-sectional scanning electron micrograph (SEM) of the completed device is shown in Fig. 1b. This corresponds to a $1 \mu\text{m}$ -wide stripe structure. Contrast between the GaAs, $\text{Al}_{0.42}\text{Ga}_{0.58}\text{As}$ and InGaP

layers is observed, although the quantum wells and thin GaAs insertions are not resolved. The image is indicative of the excellent, defect-free regrowth quality.

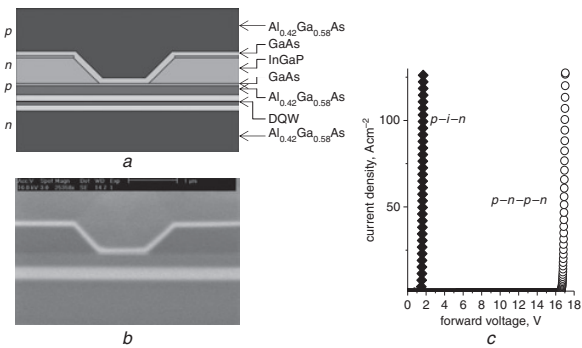


Fig. 1 Schematic diagram of self-aligned stripe; cross-sectional SEM of regrown structure; and current density against voltage characteristics of mesa diodes from *p-i-n* (solid circles) and *p-n-p-n* (open circles) portions of the wafer

a Schematic of self-aligned stripe
b SEM of regrown structure
c Current density against voltage characteristics

To characterise the electrical characteristics of the current blocking layers, $100 \mu\text{m}$ -diameter circular mesas were processed from portions of the wafer where the InGaP was removed (*p-i-n* structure) and where the InGaP is left intact (*p-n-p-n* structure). Fig. 1c shows the current density against voltage for these two devices. The *p-i-n* devices exhibit typical diode characteristics, turning on at ~ 1.5 V. The *p-n-p-n* device exhibits effective current blocking, with a breakdown of the current blocking evidenced by the large increase in current >17 V. At forward voltages <17 V current flow should therefore be confined to the stripe region.

Results: Fig. 2a shows the CW output power against drive current for a laser with a $3 \mu\text{m}$ -wide stripe in the InGaP, together with a corresponding lasing electroluminescence (EL) spectrum in Fig. 2c. The threshold current is 20 mA, corresponding to a threshold current density (J_{th}) of 666 Acm^{-2} , calculated without taking into account any current spreading and hence provides an upper limit to the value for J_{th} . The maximum CW output power from one facet is 98 mW (limited by thermal rollover), with 0.3 W/A per facet slope efficiency. Devices were tested up to 90°C (Fig. 2b), where CW operation was still achieved (with no active cooling). A characteristic temperature, T_0 of 150 K is extracted over the range 10 – 50°C . The above threshold EL spectrum exhibits a Fabry-Pérot lasing envelope at a central wavelength of 994 nm, with no obvious competition from higher order lateral modes observable in the spectrum (inset).

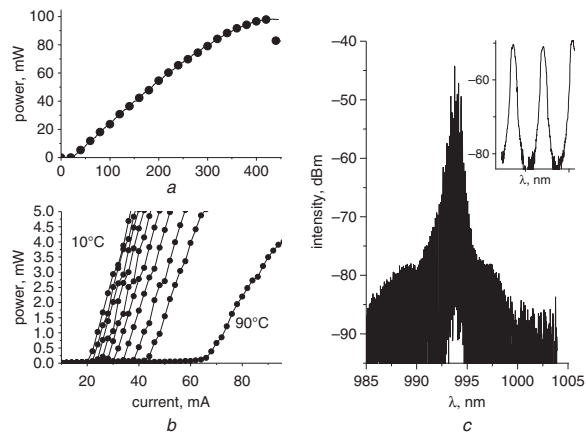


Fig. 2 CW output power against current for $3 \mu\text{m}$ -wide stripe laser, demonstrating maximum output power of 98 mW (Fig. 2a), and for range of temperatures 10 – 90°C (Fig. 2b); lasing spectrum at 40 mA CW (Fig. 2c)

Fig. 3 shows the horizontal and vertical far-field profiles of the device for low current (40 mA) (Fig. 3b) and high current (400 mA) (Fig. 3c), recorded by coupling the light into a standard far-field goniometer with InGaAs detector. The measured low current divergence angles of 33° vertical and 14.6° horizontal correlate well with those predicted using Fimmwave software [7] (Fig. 3a) of 33.3° and 14.4° . The difference in far-field parameters is attributed to uncertainties in the $\text{Al}_x\text{Ga}_{1-x}\text{As}$ composition owing to regrowth on a patterned surface. The wider divergence at higher currents is attributed to an enhanced contribution from gain guiding. The device operates on the fundamental lateral mode under all injection conditions, even up to the maximum output power at 400 mA. Such single lateral mode behaviour is further evidenced through scanning a lensed singlemode optical fibre to obtain the near-field profile. The near-field profile (Fig. 3d) exhibits a single peak, with the cone of light originating from a single $\sim 3 \times 2 \mu\text{m}$ section of the device, in the centre of the $50 \mu\text{m}$ -wide ridge. However, resolution is of the order of $\sim 2 \mu\text{m}$ (limited by the lensed fibre) so, whilst detailed mapping of the near-field is not possible, the measurement demonstrates the effective current and optical confinement within the device.

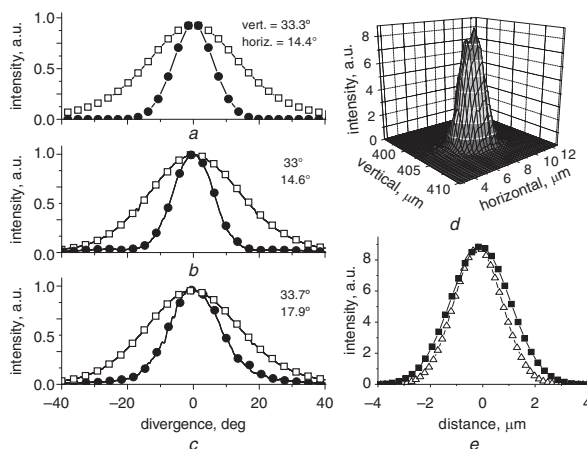


Fig. 3 Normalised far-field profiles of device (Figs. 3a–c)

- a Modelled
- b Measured at 40 mA
- c Measured at 400 mA with emission from fundamental mode only
- FWHM of the vertical and horizontal far-fields are indicated
- d Experimentally measured near-field profile for which resultant horizontal (closed squares) and vertical (open triangles) near-field sections are extracted in (Fig. 3e)

Conclusions: We have demonstrated a novel GaAs-based self-aligned laser utilising an InGaP current blocking and optical confinement layer. This single overgrowth design offers a simple, manufacturable method for single lateral mode lasers on GaAs substrates.

© The Institution of Engineering and Technology 2008

13 May 2008

Electronics Letters online no: 20081236

doi: 10.1049/el:20081236

K.M. Groom, B.J. Stevens, D.T. Childs, R.R. Alexander, A.B. Krysa, J.S. Roberts and R.A. Hogg (The EPSRC National Centre for III-V Technologies, Department of Electronic & Electrical Engineering, The University of Sheffield, Centre for Nanoscience & Technology, North Campus, Broad Lane, Sheffield S3 7HQ, United Kingdom)

E-mail: k.m.groom@sheffield.ac.uk

A.S. Helmy (Department of Electrical & Computer Engineering, University of Toronto, 10 King's College Rd., Toronto, ON M5S 3G4, Canada)

References

- 1 Nishi, H., Yano, M., Nishitani, Y., Akita, Y., and Takusagawa, M.: 'Self-aligned structure InGaAsP/InP DH lasers', *Appl. Phys. Lett.*, 1979, **35**, (3), pp. 232–234
- 2 Yeh, N.T., Liu, W.S., Chen, S.H., Chiu, P.C., and Chyi, J.I.: 'InAs/GaAs quantum dot lasers with InGaP cladding layer grown by solid source molecular beam epitaxy', *Appl. Phys. Lett.*, 2002, **80**, (4), pp. 535–537
- 3 Kish, F.A., Caracci, S.J., Holonyak, Jnr N., Dallesasse, J.M., Hsieh, K.C., and Ries, M.J.: 'Planar native-oxide index-guided $\text{Al}_x\text{Ga}_{1-x}\text{As}$ quantum well heterostructure lasers', *Appl. Phys. Lett.*, 1991, **59**, (14), pp. 1755–1757
- 4 Nido, M., Komazaki, I., Kobayashi, K., Endo, K., Ueno, M., Kamejima, T., and Suzuki, T.: 'AlGaAs/GaAs self-aligned LD's fabricated by the process containing vapour phase etching and subsequent MOVPE regrowth', *IEEE J. Quantum Electron.*, 1987, **23**, (6), pp. 720–724
- 5 Mawst, L.J., Yang, H., Nesnidal, M., Al-Muhanna, A., Botez, D., Vang, T.A., Alvarez, F.D., and Johnson, R.: 'High-power, single mode, Al-free InGaAsP/InGaP/GaAs distributed feedback diode lasers', *J. Cryst. Growth*, 1998, **195**, pp. 609–616
- 6 Ishikawa, S., Kukagai, K., Chida, H., Miyazaki, T., Fuji, H., and Endo, K.: '0.98–1.02 μm strained InGaAs/AlGaAs double quantum well high-power lasers with GaInP buried waveguides', *IEEE J. Quantum Electron.*, 1993, **29**, (6), pp. 1936–1942
- 7 Fimmwave software by Photon Design, <http://www.photond.com>